Bioorganic & Medicinal Chemistry Letters 23 (2013) 6228–6233

Contents lists available at ScienceDirect

Bioorganic & Medicinal Chemistry Letters

journal homepage: www.elsevier.com/locate/bmcl

# Discovery and optimization of orally active cyclohexane-based prolylcarboxypeptidase (PrCP) inhibitors

John S. Debenham [a,*], Thomas H. Graham [a], Andreas Verras [a], Yong Zhang [a], Matthew J. Clements [a], Jeffrey T. Kuethe [b], Christina Madsen-Duggan [a], Wensheng Liu [a], Urmi R. Bhatt [c], Dunlu Chen [c], Qing Chen [d], Margarita Garcia-Calvo [c], Wayne M. Geissler [c], Huaibing He [d], Xiaohua Li [d], JeanMarie Lisnock [e], Zhu Shen [c], Xinchun Tong [d], Elaine C. Tung [d], Judyann Wiltsie [e], Suoyu Xu [d], Jeffrey J. Hale [a], Shirly Pinto [c], Dong-Ming Shen [a]

[a] Department of Medicinal Chemistry, Merck Research Laboratories, PO Box 2000, Rahway, NJ 07065-0900, USA
[b] Department of Process Chemistry, Merck Research Laboratories, PO Box 2000, Rahway, NJ 07065-0900, USA
[c] Department of Metabolic Disorders, Merck Research Laboratories, PO Box 2000, Rahway, NJ 07065-0900, USA
[d] Department of Drug Metabolism, Merck Research Laboratories, PO Box 2000, Rahway, NJ 07065-0900, USA
[e] Department of In Vitro Sciences, Merck Research Laboratories, PO Box 2000, Rahway, NJ 07065-0900, USA

ARTICLE INFO

*Article history:*
Received 9 September 2013
Accepted 30 September 2013
Available online 8 October 2013

*Keywords:*
PrCP
Prolylcarboxypeptidase
Serine protease
Inhibitor
Obesity

ABSTRACT

The synthesis, SAR, binding affinities and pharmacokinetic profiles are described for a series of cyclohexane-based prolylcarboxypeptidase (PrCP) inhibitors discovered by high throughput screening. Compounds show high levels of ex vivo target engagement in mouse plasma 20 h post oral dose.



Prolylcarboxypeptidase (PrCP) is a lysosomal carboxypeptidase. This serine protease cleaves the amide bond between a C-terminal amino acid and a proline residue (i.e., peptide-Pro-Xxx-OH), and degrades angiotensins II and III,[1] plasma prekallikrein[2] and α-melanocyte stimulating hormone (α-MSH).[3] It is found in many tissues including liver, kidney, pancreas, heart, brain, adipose, hypothalamus and gut and extracellularly in plasma and urine.[4] PrCP has been implicated in several biological functions including cardiovascular,[5] inflammation,[6] and food intake regulation.[3] The previous lack of small molecule tools to interrogate PrCP function in vivo has made it difficult to confirm these findings and also assess its potential utility as a therapeutic target.

Our laboratories have recently disclosed several small molecule tools to evaluate PrCP inhibition for the modulation of feeding behavior and weight gain in mouse obesity models (Fig. 1).[7–9]

The first tool compound our laboratories identified was **1**. When evaluated in a 5 day PrCP wild-type (WT) knock-out (KO) mouse weight loss study at 100 mg/kg, the WT showed a 4.9% decrease in body weight. The KO mice showed a 1% decrease in body weight indicating that some off-target activity was in play as well, but these results were promising.[7] Compound **1** had a low bioavailability of 13% with a clearance of 23 mL/min/kg. Compound **2** was designed to reduce structural complexity of **1** by the removal of one of the chiral centers of the original lead. Potency was maintained, but at the expense of bioavailability moving from 13% for **1** to just 4% with **2**. In order to evaluate it in a similar PrCP WT/KO mouse weight loss model a subcutaneous constant infusion pump was required. Dosing for 7 days at 12 mg/kg resulted in weight loss that was equivalent between WT and KO animals again indicating an off-target activity was in play.[8] The third tool evaluated **3** was designed to differentiate itself by removal of the dichlorobenzimidazole substituted pyrrolidine component of the previous series. Additionally, this compound had considerably more CNS exposure, something that was postulated to be required for enhanced weight loss effects past what was observed in the first study. Like **2**, **3** had inadequate oral exposure requiring it to be dosed with a continuous infusion pump. At 30 mg/kg non-mechanism based weight loss was again observed with significant skin related AEs at the injection site due to compound precipitation around the point of infusion.[9a]

* Corresponding author. Tel.: +1 908 740 5497; fax: +1 908 740 3132.
*E-mail address:* john_debenham@merck.com (J.S. Debenham).

0960-894X/$ - see front matter © 2013 Elsevier Ltd. All rights reserved.
http://dx.doi.org/10.1016/j.bmcl.2013.09.094

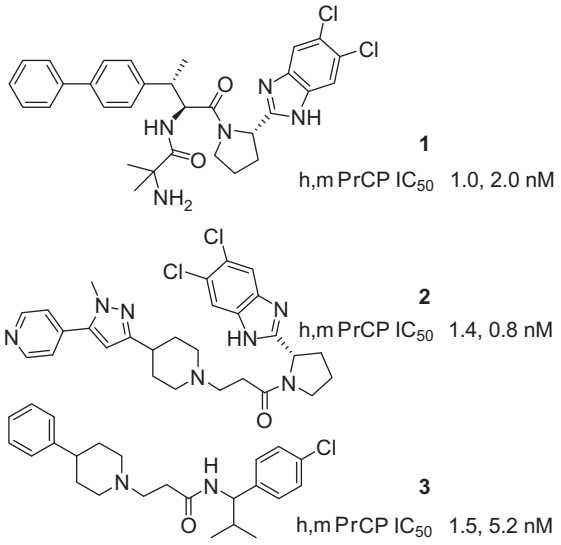


**Figure 1.** Early PrCP lead compounds; h = human, m = mouse.

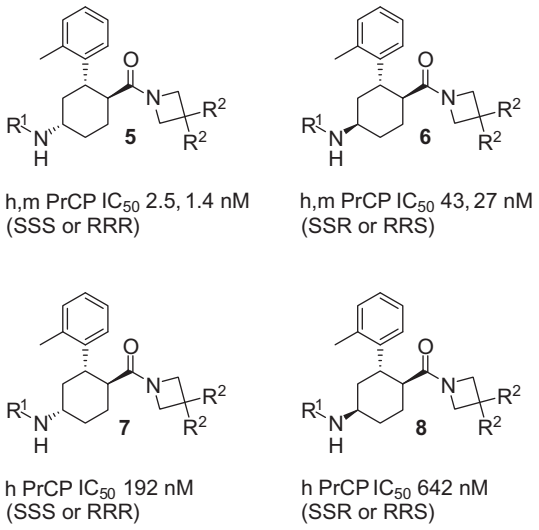


**Figure 3.** Stereochemical deconvolution of PrCP activity. $R^1$ = 4-chlorobenzyl, $R^2$ = phenyl.

Our objective evolved to find a structurally distinct scaffold that could generate tools with improved oral exposure suitable for in vivo biological evaluation in mice and that could then serve as a platform for further lead optimization. A high throughput screen (HTS) of the Merck sample collection was carried out. One of the hits obtained was isomeric mixture **4** as trans cinnamide-derived racemates and a mixture of diastereomers at the benzylamine substitution (Fig. 2). It showed 200 nM $IC_{50}$ human (h) PrCP activity despite being a mixture of stereoisomers. In order to determine the biological properties of the most active isomer an intermediate used in the preparation of **4** was resolved by chiral HPLC and all the trans isomers were prepared (Fig. 3). The isomer bearing an axially oriented benzylamino group **5** showed potent activity for human (h) and mouse (m) PrCP activity at 2.5 and 1.4 nM $IC_{50}$, respectively, with the other isomers showing 10–300-fold less activity. With the serendipitous **5** in hand, its off target activity was evaluated to benchmark potential strengths and shortcomings of the new scaffold. Compound **5** was shown not to be a significant inhibitor of the cytochrome p450 enzymes ($IC_{50}$ in μM): CYP3A4 25, CYP2C9>50, and CYP2D6 20. Human PXR activity was also minimal with an $EC_{50}$ of >15 μM. The ion channel activity of **5** was less optimal. In the hERG potassium channel assay the activity was determined to be about 3 nM binding $IC_{50}$. Not surprisingly, based on the hydrophobic nature of **5** (Log*P* 8.04),[10] the compound had essentially unmeasurable free fraction in both human and mouse plasma. Compound **5** was screened broadly against a customized panel of radioligand binding and enzymatic assays to examine other potential off target activites.[11] Of note, it showed activity at human CB1R of 345 nM $IC_{50}$. CB1R activity is known to strongly influence feeding behavior and body weight changes across a wide variety of species including humans. As a tool compound to interrogate biological activity including feeding behavior, this CB1 activity would need to be minimized in order to allow a more direct interpretation of observed in vivo activity.

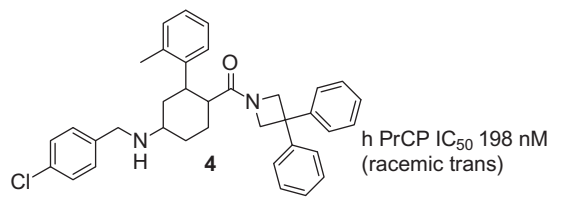


**Figure 2.** PrCPi screening hit.

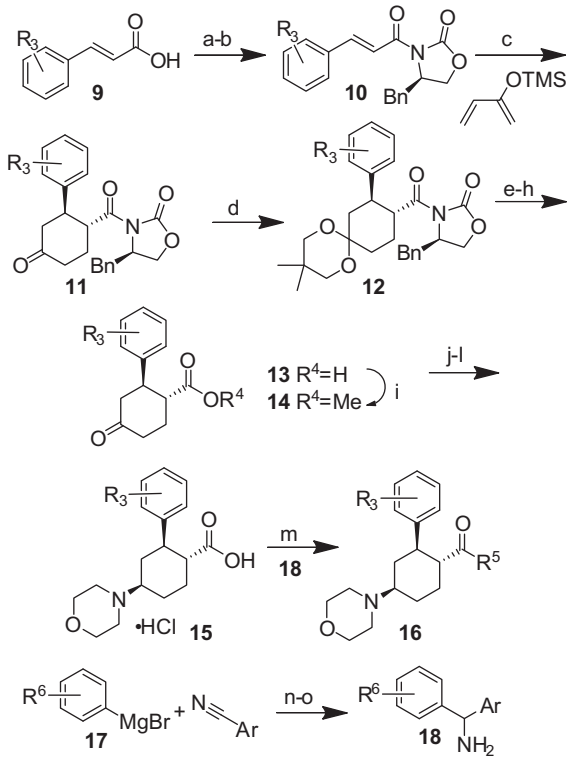


**Scheme 1.** Methods to prepare compounds of general structure **16**. Reagents and conditions: (a) oxalyl chloride, $CH_2Cl_2$, rt; (b) *n*-BuLi, (*R*)-4-benzyloxazolidin-2-one, THF, −78 °C; (c) diethylaluminum chloride, $CH_2Cl_2$, 0 °C to rt, 40–50% steps a–c; (d) 2,2-dimethylpropane-1,3-diol, *p*-TsOH, toluene, reflux, THF; (e) LiOH, $H_2O_2$, $H_2O$, THF, 0 °C to rt; (f) HCl (aq), 60 °C; (g) dicyclohexylamine, MTBE, rt; (h) $NaHSO_4$ (aq), rt, steps d–h 81%; (i) $(CH_3)_3SiCHN_2$, benzene:MeOH (7:1) ⩾99%; (j) morpholine (2 equiv), $Ti(O\text{-}iPr)_4$ (2 equiv), $CH_2Cl_2$ (0.4 M), rt, then $NaCNBH_3$ (8 equiv), MeOH, HCl (8 equiv) −78 °C to rt, slowly (6–7 h), ~89% isomer **16**, ~10% alternate isomer (not shown); (k) LiOH, $H_2O$, 70 °C, 24 h; (l) acetone, $H_2O$, HCl, ⩾99%; (m) HATU, DIEA, DMA, amine, rt, 7–70%; (n) THF, 0 °C or rt; (o) MeOH or THF/MeOH, $NaBH_4$, 25–80%.

In order to access structurally optimal diastereomers an asymmetric synthesis of the 4-oxo-2-phenylcyclo-hexanecarboxylic acid core **13** was devised employing the methods of Evans et al.[12]

**Table 1**
PrCP inhibition and binding affinities of compounds at human and mouse PrCP inhibition and human hERG (IKr) binding expressed as $IC_{50}$ (nM)

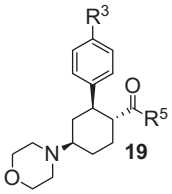


| Compound | $R_4$[a] | PrCP(h, m)[b] $IC_{50}$, nM | hERG $IC_{50}$, nM |
|---|---|---|---|
| **20** | 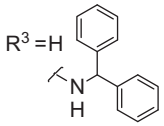 | 29, 180 | 170 |
| **21** | 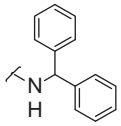 | 2.5, 12 | 530 |
| **22** (CB1 = 8600) | 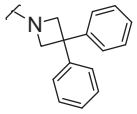 | 1.2, 6.6 | 290 |
| **23** | 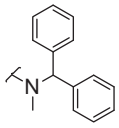 | 17, 170 | NA |
| **24** | 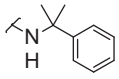 | 440, NA | NA |
| **25** | 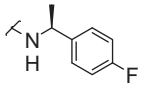 | 12, 320 | 2200 |
| **26** | 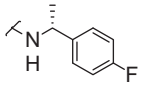 | 480, NA | NA |
| **27** | 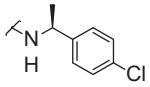 | 3.0, 44 | NA |

[a] $R^3$ = Br unless otherwise indicated.
[b] Values are based on one or two experiments, each in triplicate.

(Scheme 1). Starting from commercially available substituted phenylprop-2-enoic acids and the (4*R*)-4-benzyl-1,3-oxazolidin-2-one chiral auxiliary, oxazolidinone dienophile **10** was prepared, and subsequently subjected to a Diels–Alder cycloaddition reaction to form the core 4-oxo-2-phenylcyclohexanecarboxylate **11**. In order to remove the chiral auxiliary, compounds such as **11** are typically treated with aqueous LiOH and $H_2O_2$. However, the presence of the ketone was not compatible with those conditions, and required protection as the cyclic acetal **12**. Once protected, the auxiliary on **12** was hydrolyzed. Subsequent deprotection of the acetal with HCl afforded the free acid **13**. It was found that this intermediate was readily purified by formation of the dicyclohexylamine salt in EtOAc. Following the salt break of purified **13** with $NaHSO_4$, the acid was protected as the methyl ester. Reductive amination of the ketone was carried out with morpholine mediated by Ti(O-*i*-Pr)$_4$ at room temperature for 15 h in $CH_2Cl_2$ followed by subsequent addition of $NaCNBH_3$ in MeOH at −78 °C and then methanolic HCl at −78 °C. The reaction mixture was gradually warmed to rt over 7 h to afford the desired R amine isomer in a 9:1 ratio with the less active (*S*) isomer as the minor product. When the reaction was warmed more quickly, over 3–4 h, for example, the selectivity was observed to drop giving the preferred isomer in a reduced 4–5:1 selectivity. The protection of **13** as the methyl ester facilitated the isolation and purification of the intermediate amino ester by silica gel flash chromatography in bulk. Hydrolysis of the ester followed by activation of the acid for amide coupling with HATU and subsequent reaction with the various amines in the presence of DIEA afforded the final compounds of general formula **16**. When the amines employed in the amide coupling reaction of Scheme 1 are not commercially available biaryl or aryl-heteroaryl, the methods of Terrasson et al. were employed in their construction.[13] In the first step, a substituted aryl Grignard reagent was reacted with substituted benzonitrile in THF. Once the initial addition was complete the solvent was either exchanged with MeOH or the reaction is diluted with MeOH so that the reduction of the intermediate imine can be completed with $NaBH_4$ providing the amine that was the coupling partner to acid **15**.

Human and mouse PrCP enzyme inhibition was determined using a standard protocol that was previously described.[7,8] In single enantiomer cases the listed data are for the eutomers, which

**Table 2**
Binding affinities of compounds at human and mouse PrCP and human hERG (IKr) expressed as $IC_{50}$ (nM)

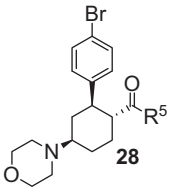


| Compound | $R_4$ | PrCP(h, m)[a] $IC_{50}$, nM | hERG $IC_{50}$, nM |
|---|---|---|---|
| **29** | 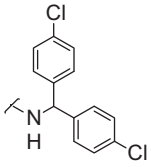 | 2.6, 3.4 | 39 |
| **30** | 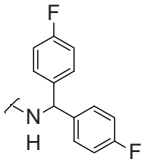 | 0.66, 1.4 | 100 |
| **31** | 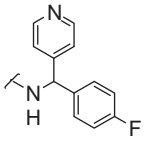 | 0.60, 3.0 | 8400 |
| **32** | 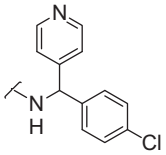 | 0.18, 0.74 | 1900 |
| **33** | 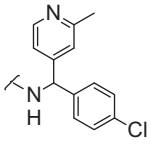 | 2.2, 10 | 1500 |
| **34** | 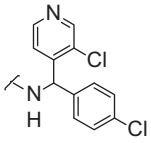 | 2.7, 8.6 | 690 |
| **35** | 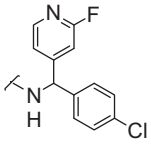 | 0.079, 0.28 | 590 |
| **36** | 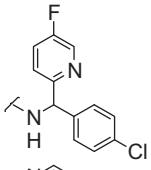 | 0.95, 1.7 | 180 |
| **37** | 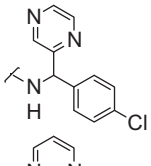 | 4.6, 14 | 1000 |
| **38** | 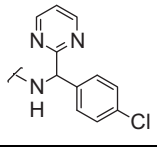 | 36, 210 | 1200 |

[a] Values are based on one or two experiments, each in triplicate; Data are for the more potent single enantiomer; absolute stereochemistry was not determined.

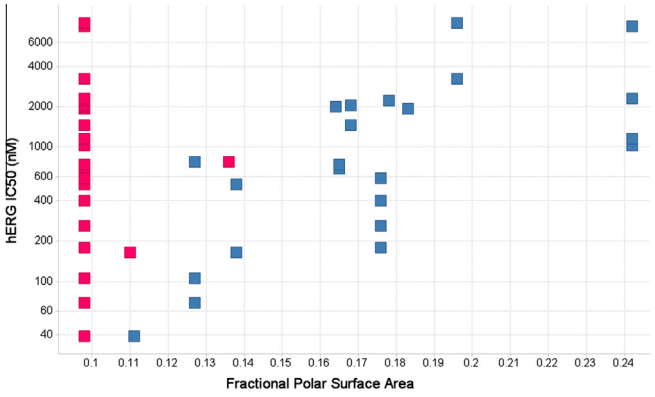


**Figure 4.** Fragment fractional polar surface area versus hERG $IC_{50}$. Fractional PSA for fragmented molecules. Biaryl (right portion) fragments are indicated in blue. Substituted cyclohexyl (left portion) fragments are indicated in red. $IC_{50}$ values are calculated in an MK499 displacement assay.

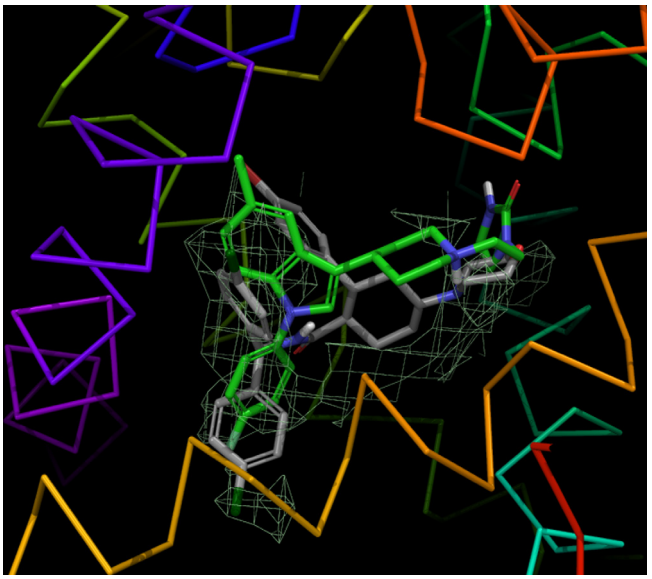

**Figure 5.** Hydrophobicity map and overlay with sertindole. hERG residues are indicated with a ribbon model colored by sequence position. Compound **29** is represented with grey carbons and sertindole is represented with green carbons. Hydrophobicity maps 2 Å around the ligand are indicated in light green.

are typically 10–100-fold more potent than the corresponding distomers. Our initial goal was to evaluate structures of reduced lipophilicity. It was anticipated that as compound polarity increased we would see free fraction move to measureable amounts, and also potential decreased CB1 activity. The 4-chlorobenzyl domain of **6** was exchanged with several amines[14] and it was found that morpholine maintained potency, while decreasing MW and lipophilicity. Table 1 shows a variety of analogs that were prepared exploring reduction of complexity and molecular weight from lead compound **5** which had a MW of 549 and a Log*P* of 8.04.[15] Compound **20** shows the move from the diphenyl azetidine amide to the benzhydryl amide and removal of the ortho methyl group of **5**. **20** lost about 12-fold activity for human PrCP and about 129-fold for mouse activity. Installation of a para bromo group **21** on the phenyl at the 2-position brought back the human activity of **5** and mouse activity was within ninefold of **5** at 12 nM. Moreover hERG activity was attenuated 177-fold from 3 to 530 nM $IC_{50}$. N-methylation of the amide nitrogen of **21** was detrimental to both mouse and human activity with **23** displaying 7 and 14-fold loss of potency, respectively. Comparing diphenyl azetidine amide **22**

**Figure 6.** Predicted binding mode of **29**. Close up of **29** and select residues within 4.5 Å of the ligand.

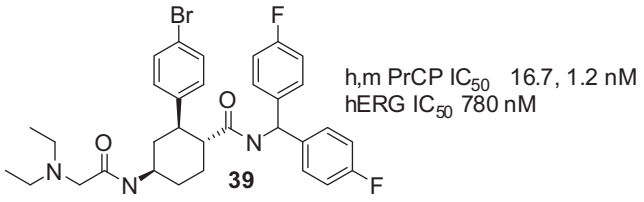


**Figure 7.** Non-morpholino analog **39**.

**Table 3**
Pharmacokinetic profiles of select compounds

| Compd | %F | $t_{½}$ (h) | AUCNpo (μM h kg/mg) | PPB[a] |
|---|---|---|---|---|
| **37** | 5.2 | 1.2 | 0.010 | — |
| **31** | 6.9 | 2.0 | 0.019 | 2.1 |
| **32** | 8.9 | 1.4 | 0.016 | 1.9 |
| **34** | 17 | 1.5 | 0.049 | — |
| **39** | 32 | 6.5 | 0.59 | — |
| **21** | 36 | 3.1 | 0.19 | 3.2 |
| **36** | 50 | 4.9 | 0.46 | 1.8 |
| **30** | 77 | 7.6 | 0.92 | 0.5 |
| **35** | 90 | 2.9 | 0.56 | 1.9 |

[a] Plasma protein binding data reported as % unbound in 100% C57BL/6 mouse plasma.

with **5**, the presence of the morpholine amine and bromo phenyl group allow retention of activity and almost a 100-fold shift in hERG activity to 290 nM $IC_{50}$. Moreover the human CB1R activity attenuates 25-fold from 345 nM $IC_{50}$ to 8600 nM. Cumyl amide **24** showed a 176-fold loss of human PrCP activity relative to screening lead **5**. However removal of one of the cumyl methyl groups and substitution with either para F or Cl returned most of the human activity of lead **5** with the S amide enantiomers. Of note was the R enantiomer **26** that showed a 40-fold drop in activity. Also, of the active S enantiomers the mouse potency was shifted 14–26-fold less active than human versus **5** that had no such shift. At this point it was clear the extra aryl group was providing enhanced mouse potency. Table 2 shows more elaborated benzhydryl derivatives both with achiral and chiral amides. Parahalogenated **29** and **30** showed more parity between human and mouse with the difluoro **30** showing this first significant improvement from the original lead. While **30** has an unfavorable hERG activity (100 nM), it still had an improved hERG/PrCP activity ratio of 150:1 versus the non-selective **5** which was about 1:1.

As stated earlier, lead compound **5** possessed very potent hERG activity. In order to evaluate compound features and properties contributing to hERG ion channel binding, we calculated several physical properties in Pipeline Pilot including polar surface area (PSA) and fractional PSA (PLP v. 7.5.2, Accelrys). To explore the features of our ligands effecting hERG affinity, compounds were split into two fragments at the amide bond. Fragments were then neutralized and hydrogens were added. This resulted in fragments that contain the biaryl portion (right) and fragments that contain the more polar substituted cyclohexyl portion (left). PSA was calculated for all fragments using the 2D method of Ertl implemented in PLP.[16] Figure 4 illustrates a clear dependence of hERG binding on fractional PSA, particularly on the biaryl portion of the molecules. Compounds with increased polarity proportional to their size in the biaryl region of the molecule, display significantly less hERG affinity. Small modifications resulting in an approximately 10% increase in polarity on the right side alone can attenuate hERG binding affinity by greater than 100-fold. While there may be some hERG binding dependency on the left side of the molecule, the structural diversity in this region does not allow such conclusions.

To elucidate atomic features that drive hERG activity we also generated a putative binding mode to hERG homology models. Initially we used an in house structure generated from a KcsA template containing a high potency hERG inhibitor MK499.[17] This homology model is of the closed form of the channel, wherein the pore channel is narrowed and thought to be in an inactive state. Ligand docking was done with Glide[18] using a grid prepared with decreased Van der Waals radii of 0.8 to allow for an increase in the number of poses; however, given the size of the active site relative to our compounds we were unable to generate a satisfactory binding mode. Furthermore, alignment of our compounds with MK499 was poor due to discrepancies between aromatic and cation features in the ligands hypothesized to be important in binding (data not shown).

To overcome these issues we used coordinates for the hERG channel homology model from the Åqvist group that was built using a KvAP structural template (pdbid 2A0L).[19] This structure was based on the open form of the channel and features docked poses for ligands that share significant 3D shape to our series.[20] Compound **29** was docked into the hERG homology model using Glide with default settings. We found a very similar binding mode to the sertindole ligand (Fig. 5). Representation of the grid surface using a hydrophobicity surface in Maestro indicated that the aryl groups occupy a lipophilic region consistent with the PSA dependent SAR. The biaryl groups lie in a region bordered by hydrophobic and aromatic residues including F656 and F652

**Table 4**
Mouse ex vivo target engagement (TE) assay results

| Compd | p.o. dose[a] (mg/kg) | $[compd]_{plasma}$ (nM) | $K_i$ (100%)[b] (nM) | TE[c] (%) |
|---|---|---|---|---|
| **30** | 30 | 1025 | 70.5 | 90.9 |
| **36** | 30 | 1837 | 158 | 92.9 |
| **39** | 30 | 2883 | 19.0 | 99.9 |
| **35** | 30 | 390 | 1.10 | ⩾100 |
| **35** | 10 | 163 | 1.10 | 98.2 |

[a] Fasted lean male C57 mice ($n = 3$) were dosed by oral gavage, samples collected at 20 h post-dose, citrate treated blood (1:3 blood/0.1 M disodium citrate) was prepared for LC/MS analysis by protein precipitation with acetonitrile.

[b] Calculated $K_i$ in 100% mouse plasma. The inhibition of PrCP in the presence of 25% plasma was measured and extrapolated to 100% plasma using data from 0% plasma in the primary assay. The assay used heat-inactivated plasma to minimize the activity of non-PrCP proteases.

[c] Inhibition was measured in 100% mouse plasma that was heat-inactivated to minimize the protease activity.

(Fig. 6). L650 further contributes to the lipophilicity in this region. One clear hydrogen bond is evidently made from S649 to the morpholine oxygen. SAR supporting this interaction is evidenced by the decreased potency of **39** which is unable to make this contact.[21]

These observations that increased fractional polar surface area directly related to decreased hERG affinity corresponded well with our desire to reduce the hydrophobicity of lead compound **5**. Examining some of the more polar analogs in Table 2 showed that the unsubstituted pyridine analogs **31** and **32** both showed a marked decrease in hERG affinity to 8400 and 1900 nM, respectively, while also maintaining or slightly increasing potency (**32**). For **31** and **32** the hERG to hPrCP ratio has increased to over 10,000:1. Pyrimidine and pyrazine analogs had the most fractional polar surface area, but also lost considerable PrCP activity.

The compound of greatest interested to us in Table 2 was **35**, which showed exceptional human and mouse potency of 0.079 and 0.28 nM $IC_{50}$, respectively. While the 590 nM $IC_{50}$ hERG activity would indicate the compound would have questionable value for human development it would not present a problem as a tool for the use in mouse since hERG does not play a major role in cardiac repolarization in mice like it does in humans. Substituted pyridine or pyridine isomer analogs **33**, **34**, and **36** showed good parity between human and mouse activity of between 1 and 10 nM $IC_{50}$. Compound **39** in Figure 7 shows the effect of moving the basic amine further from the cyclohexane ring. While potency can be maintained for mouse at 1 nM the parity between mouse and human decreases with 14-fold less activity at human PrCP.

Several compounds were selected for further profiling in mouse. In terms of their pharmacokinetic profiles (Table 3), pyrazine **37**, and unsubstituted pyridines **31**, **32**, and 3-chloro substituted pyridine **34** showed poor bioavailability at 5–17% with low oral exposure. Considerable improvements in %F were noted as the heterocycle was replaced with phenyl **39**, **21**, and **30** or 2-substituted pyridine **36**. 2-Fluropyridine **35** had the highest bioavailability at 90% with good oral exposure and 1.9% unbound fraction in mouse plasma. A select group of these compounds were subsequently evaluated for ex vivo target engagement (TE) using methods described by our laboratories previously (Table 4).[22] Here compounds were dosed orally and plasma samples were collected 20 h post dosing to assess TE. A single 30 mg/kg oral dose was able to achieve ~90% TE in plasma using compounds **30** and **36**. The improved $K_i$ values of **39** and **35** in 100% mouse plasma allowed them to achieve complete (**35** at 30 mg/kg) or near complete target engagement (**35** at 10 mg/kg or **39** at 30 mg/kg). Structurally differentiated from our earlier leads **1**–**3**, compounds **35** and **39** maintain high levels of TE and can be orally administered. Based on the above results, these cyclohexane based PrCP inhibitors could be used as tools to further elucidate the potential utility and biological actions of PrCP inhibition in vivo.

## References and notes


1. (a) Odya, C. E.; Marinkovic, D. V.; Hammon, K. J.; Stewart, T. A.; Erdos, E. G. *J. Biol. Chem.* **1978**, *253*, 5927; (b) Yang, H. Y. T.; Erdos, E. G.; Chiang, T. S.; Jenssen, T. A.; Rodgers, J. G. *Biochem. Pharmacol.* **1970**, *19*, 1201.
2. (a) Shariat-Madar, Z.; Mahdi, F.; Schmaier, A. H. *Blood* **2004**, *103*, 4554; (b) Shariat-Madar, Z.; Mahdi, F.; Schmaier, A. H. *J. Biol. Chem.* **2002**, *277*, 17962; (c) Moreira, C. R.; Schmaier, A. H.; da Mahdi, F.; Motta, G.; Nader, H. B.; Shariat-Madar, Z. *FEBS Lett.* **2002**, *523*, 167.
3. (a) Jeong, J. K.; Diano, S. *Trends Endocrin. Met.* **2013**, *24*, 61; (b) Jeong, J. K.; Szabo, G.; Raso, G. M.; Meli, R.; Diano, S. *Am. J. Physiol. Endocrinol. Metab.* **2012**, *302*, E1502; (c) Diano, S. *Front. Neuroendocrin.* **2011**, *32*, 70; (d) Wallingford, N.; Perroud, B.; Gao, Q.; Coppola, A.; Gyengesi, E.; Liu, Z.-W.; Gao, X.-B.; Diament, A.; Haus, K. A.; Shariat-Madar, Z.; Mahdi, F.; Wardlaw, S. L.; Schmaier, A. H.; Warden, C. H.; Diano, S. *J. Clin. Invest.* **2009**, *119*, 2291; (e) Rabey, F. M.; Gadepalli, R. S. V. S.; Diano, S.; Cheng, Q.; Tabrizian, T.; Gailani, D.; Rimoldi, J. M.; Shariat-Madar, Z. *Curr. Med. Chem.* **2012**, *19*, 4194.
4. (a) Skidgel, R. A.; Erdos, E. G. *Immunol. Rev.* **1998**, *161*, 129; (b) Kumamoto, K.; Stewart, T. A.; Johnson, A. R.; Erdos, E. G. *J. Clin. Invest.* **1981**, *67*, 210; (c) Yang, H. Y. T.; Erdos, E. G.; Chiang, T. S. *Nature* **1968**, *218*, 1224; (d) Miller, J. J.; Changaris, D. G.; Levy, R. S. *Life Sci.* **1991**, *48*, 1529.
5. (a) Adams, G. N.; LaRusch, G. A.; Stavrou, E.; Zhou, Y.; Nieman, M. T.; Jacobs, G. H.; Cui, Y.; Lu, Y.; Jain, M. K.; Mahdi, F.; Shariat-Madar, Z.; Okada, Y.; D'Alecy, L. G.; Schmaier, A. H. *Blood* **2011**, *117*, 3929; (b) Mallela, J.; Yang, J.; Shariat-Madar, Z. *Int. J. Biochem. Cell Biol.* **2009**, *41*, 477; (c) Wang, L.; Feng, Y.; Zhang, Y.; Zhou, H.; Jiang, S.; Niu, T.; Wei, J. L.; Xu, X.; Xu, X. P.; Wang, X. *Am. J. Obstet. Gynecol.* **2006**, *195*, 162.
6. (a) Chajkowski, S. M.; Mallela, J.; Watson, D. E.; Wang, J.; McCurdy, C. R.; Rimoldi, J. M.; Shariat-Madar, Z. *Biochem. Biophys. Res. Commun.* **2011**, *405*, 338; (b) Ngo, M. L.; Mahdi, F.; Kolte, D.; Shariat-Madar, Z. *J. Inflamm.* **2009**, *6*, 3.
7. Zhou, C.; Garcia-Calvo, M.; Pinto, S.; Lombardo, M.; Feng, Z.; Bender, K.; Pryor, K. D.; Bhatt, U. R.; Chabin, R. M.; Geissler, W. M.; Shen, Z.; Tong, X.; Zhang, Z.; Wong, K. K.; Sinha Roy, R.; Chapman, K. T.; Yang, L.; Xiong, Y. *J. Med. Chem.* **2010**, *53*, 7251.
8. Shen, H. C.; Ding, F. X.; Zhou, C. Y.; Xiong, Y. S.; Verras, A.; Chabin, R. M.; Xu, S. Y.; Tong, X. C.; Xie, D.; Lassman, M. E.; Bhatt, U. R.; Garcia-Calvo, M.; Geissler, W.; Shen, Z.; Chen, D. L.; SinhaRoy, R.; Hale, J. J.; Tata, J. R.; Pinto, S.; Shen, D.-M.; Colletti, S. L. *Bioorg. Med. Chem. Lett.* **2011**, *21*, 1299.
9. (a) Graham, T. H.; Shen, H. C.; Liu, W.; Xiong, Y.; Verras, A.; Bleasby, K.; Bhatt, U. R.; Chabin, R. M.; Chen, D.; Chen, Q.; Garcia-Calvo, M.; Geissler, W. M.; He, H.; Lassman, M. E.; Zhu, S.; Tong, X.; Tung, E.; Xie, D.; Xu, S.; Colletti, S. L.; Hale, J. J.; Tata, J. R.; Pinto, S.; Shen, D.-S. *Bioorg. Med. Chem. Lett.* **2012**, *22*, 658; (b) Graham, T. H.; Liu, W.; Verras, A.; Reibarkh, M.; Bleasby, K.; Bhatt, U. R.; Chen, Q.; Garcia-Calvo, M.; Geissler, W. M.; Gorski, J.; He, H.; Lassman, M. E.; Lisnock, J.; Li, Z.; Zhu, S.; Tong, X.; Tung, E.; Xie, D.; Xu, S.; Xiao, J.; Hale, J. J.; Pinto, S.; Shen, D.-S. *Bioorg. Med. Chem. Lett.* **2012**, *22*, 2818.
10. Value calculated with ChemBioDraw version 12.
11. Discovery Pharmacology services provided by MDS Pharma Services, Taipei, Taiwan.
12. (a) Evans, D. A.; Chapman, K. T.; Hung, D. T.; Kawaguchi, A. T. *Angew. Chem., Int. Ed. Engl.* **1987**, *26*, 1184–1186; (b) Evans, D. A.; Chapman, K. T.; Bisaha, J. *J. Am. Chem. Soc.* **1988**, *110*, 1238–1256.
13. Terrasson, V.; Marque, S.; Scarpacci, A.; Prim, D. *Synthesis* **2006**, *11*, 1858–1862.
14. This work is not presented herein.
15. Calculated with ChemBioDraw Ultra 12.
16. Ertl, P.; Rohde, B.; Selzer, P. *J. Med. Chem.* **2000**, *43*, 3714.
17. Mitcheson, J. S.; Chen, J.; Lin, M.; Culberson, J. C.; Sanguinetti, M. C. *Proc. Natl. Acad. Sci. U.S.A.* **2000**, *97*, 12329–12333.
18. Friesner, R. A.; Banks, J. L.; Murphy, R. B.; Halgren, T. A.; Klicic, J. J.; Mainz, D. T.; Repasky, M. P.; Knoll, E. H.; Shaw, D. E.; Shelley, M.; Perry, J. K.; Francis, P.; Shenkin, P. S. *J. Med. Chem.* **2004**, *47*, 1739.
19. Stary, A.; Wacker, S. J.; Boukharta, L.; Zachariae, U.; Karimi-Nejad, Y.; Åqvist, J.; Vriend, G.; de Groot, B. L. *Chem. Med. Chem.* **2010**, *5*, 455.
20. Boukharta, L.; Keränen, H.; Stary-Weinzinger, A.; Wallin, G.; Groot, B.; Åqvist, J. *Biochemistry* **2011**, *50*, 6146.
21. For synthetic preparation see: Debenham, J.S. Shen, D.-M. Graham, T.H. Clements, M.J. Zhang, Y. Int. Pat. Appl. WO 2011146300, 2011.
22. The target engagement assay was conducted by oral dosing of mice ($n = 3$) and collection of tissue samples at 20 h post-dose. Plasma was heat-treated to eliminate endogenous protease activity. Fresh recombinant PrCP was added and the conversion of an exogenous substrate was monitored by fluorescence in a similar manner to the in vitro primary assay. Additional details can be found in: Graham, T. H.; Liu, W.; Verras, A.; Reibarkh, M.; Bleasby, K.; Bhatt, U. R.; Chen, Q.; Garcia-Calvo, M.; Geissler, W. M.; Gorski, J.; He, H.; Lassman, M. E.; Li, X.; Shen, Z.; Tong, X.; Tung, E. C.; Wiltsie, J.; Xie, D.; Xu, S.; Xiao, J.; Hale, J. J.; Pinto, S.; Shen, D.-M. *Bioorg. Med. Chem. Lett.* **2012**, *22*, 2818.